

# Non-Gaussian statistics and superdiffusion in a driven-dissipative dusty plasma

Bin Liu, J. Goree, and Yan Feng

*Department of Physics and Astronomy, The University of Iowa, Iowa City, Iowa 52242*

(Received 12 June 2008; published 22 October 2008)

Particle random motion can exhibit both anomalous diffusion and non-Gaussian statistics in some physical systems. Anomalous diffusion is quantified by a deviation from  $\alpha=1$  in a power law for a particle's mean-square displacement,  $\text{MSD} \propto (\Delta t)^\alpha$ . A deviation from Gaussian statistics for a probability distribution function (PDF) is quantified by fitting to a  $\kappa$  function or Tsallis distribution, with a fit parameter  $q$ . We report an experiment and simulations to test a theory that connects anomalous diffusion and non-Gaussian statistics. In the experiment, a single-layer dusty plasma, which behaved as a two-dimensional (2D) driven-dissipative system, had a non-Gaussian PDF. By adjusting an externally applied laser heating,  $q$  was varied over a wide range. A correlation between the deviations from Gaussian statistics and normal diffusion for a 2D liquid was found in the experiment. This correlation indicates a connection between anomalous diffusion and non-Gaussian statistics. However, such a connection is lacking in equilibrium 2D Yukawa liquids, as demonstrated in numerical simulations.

DOI: [10.1103/PhysRevE.78.046403](https://doi.org/10.1103/PhysRevE.78.046403)

PACS number(s): 52.27.Lw, 05.40.-a, 66.10.-x, 52.27.Gr

## I. INTRODUCTION

Random motion, such as Brownian motion, is traditionally described as exhibiting both normal diffusion and Gaussian statistics for fluctuating quantities [1]. However, some systems, especially nonequilibrium systems, can deviate from Gaussian statistics [2–4], or normal diffusion [5], or both. A linkage between these two traits of nonequilibrium systems, anomalous diffusion and non-Gaussian statistics, is the focus of this paper. We begin by reviewing the terminology for the two traits, and methods of measuring them.

Our approach is to analyze time series data for particle positions, i.e., particle trajectories  $\mathbf{x}(t)$ . Using these trajectories, we calculate particle displacements over time. We choose to consider a two-dimensional (2D) system, although our methods could be used also for three-dimensional (3D) systems. For long time intervals, we calculate two parameters based on the displacements. First, to determine whether motion is diffusive, a time series for the mean-square displacement (MSD) is calculated. Second, to determine whether random motion exhibits Gaussian statistics, the probability distribution function (PDF) is calculated as a histogram of particle displacements.

The PDF allows a test for Gaussian vs non-Gaussian statistics. This test is convenient for experiments that allow measuring time series for particle positions. The displacement  $|x(\tau) - x(0)|$  for each particle in a system is computed for the same time interval  $\tau$ ; we do this separately for  $x$  and  $y$ . Note that the displacement is defined so that it is always a positive value. A histogram of these displacements is then made, yielding the PDF [5]. For Brownian motion, the PDF is the positive one-half of a Gaussian function that is centered at zero. To test for non-Gaussian statistics, we determine whether the measured PDF is non-Gaussian.

While Gaussian distributions are common in the usual statistical mechanics for thermal equilibrium systems, non-Gaussian distributions also abound in many scientific and economic fields. One prominent example is the power-law tail distribution which is often observed, for example, in eco-

nomics for the price change for a given stock over a time interval [2]; in physiology for the histogram of heartbeat interval increments [3]; and in physics for the distribution of cluster sizes in self-organized critical dynamical systems [4]. Power-law tail distributions are said to have a fat tail, in comparison to a Gaussian distribution.

Power-law tail distributions are often characterized by a  $\kappa$  function. For example, in plasma physics the  $\kappa$  function sometimes accurately models a velocity distribution [6],  $f_\kappa(v) \propto (1 + v^2 / \kappa v_0^2)^{-\kappa}$ , where  $v_0$  is a characteristic speed of the distribution; this occurs in the solar wind due to weak collisionality between particles [6]. The fluctuation of magnetic field in solar wind also exhibits a power law [7]. Here,  $\kappa$  is a parameter determining the shape of the distribution function. In the limit  $\kappa \rightarrow \infty$ , the  $\kappa$  function approaches a Maxwellian-Boltzmann, i.e., Gaussian distribution. For  $\kappa$  smaller than about 10, the  $\kappa$  function has a power-law tail. One could fit an observed PDF to a  $\kappa$  function for particle displacement,

$$\{1 + \beta[|x(\tau) - x(0)|]^2 / \kappa\}^{-\kappa}, \quad (1)$$

where  $\beta^{-1}$  characterizes the width of the PDF, which always increases with  $\tau$ .

The Tsallis distribution is a power-law tail distribution that was introduced in the context of a theory for nonextensive statistical mechanics [8]. For any random variable  $z$ , the Tsallis distribution is  $[1 + \beta(q-1)z^2]^{-1/(q-1)}$ , which approaches a Gaussian for  $q=1$ , while  $q \neq 1$  indicates non-Gaussian statistics. In other words, the deviation from Gaussian statistics can be measured by the parameter  $q$ . Here, we will fit our observed PDF to a Tsallis distribution using the displacement as the random variable  $z$ ,

$$\{1 + \beta(q-1)[|x(\tau) - x(0)|]^2\}^{-1/(q-1)}. \quad (2)$$

The Tsallis distribution in Eq. (2) is the same as the  $\kappa$  function in Eq. (1), by a simple substitution of variables,  $\kappa = (q-1)^{-1}$ . It has been shown that Tsallis distributions can arise from an entire family of microscopic Langevin equations, as

a result of a specific interplay between the underlying deterministic and stochastic forces [9].

The use of the Tsallis distribution was developed as part of a theory for the statistical physics for a system that is assumed to be nonextensive. In this approach, a quantity called the generalized entropy is calculated from the probability of microstates of a system. The term nonextensive is used to describe a system where the generalized entropy is not the sum of its values for the subsystems that comprise the entire system. Assuming that a generalized entropy is maximized under the conditions of constant energy and normalization, it has been predicted that the distribution of random variables such as particle displacements will be characterized by a Tsallis distribution. Making these assumptions, the parameter  $q$  is sometimes termed a measure of nonextensivity.

Anomalous diffusion is random motion quantified by a deviation from  $\alpha=1$  in

$$\text{MSD} \propto (\Delta t)^\alpha, \quad (3)$$

where the diffusion exponent  $\alpha$  must have a positive value. Here, the mean-square displacement (MSD) is a time series for the squared displacement  $[x(\Delta t) - x(0)]^2$  averaged over all particles. Any Cartesian coordinate can be used in place of  $x$  in calculating the MSD. For a large time  $\Delta t$ , the MSD increases, often as a power law of  $\Delta t$ . Brownian motion is characterized by  $\text{MSD} \propto (\Delta t)^{1.0}$ , which is called normal diffusion, and has the property  $\alpha=1$ .

A diffusion exponent of  $\alpha \neq 1$ , on the other hand, indicates anomalous diffusion. In particular, superdiffusion, with  $\alpha > 1$ , can arise from various causes including reduced dimensionality [10–13]. Superdiffusion can also occur due to flows, for example, vortices in a liquid, but in this paper we will consider only nonflowing systems.

It has been proposed that anomalous diffusion is linked to non-Gaussian statistics [14]. In the next section we review this theory and outline our approach to test it using an experiment and simulations. We will find a correlation between the superdiffusion and non-Gaussian statistics in the experiment, which uses a nonequilibrium driven-dissipative 2D system, but not in simulations of an otherwise similar 2D equilibrium system.

## II. CONNECTING ANOMALOUS DIFFUSION AND NON-GAUSSIAN STATISTICS

### A. Tsallis relation

A theory has been proposed to model anomalous diffusion when it is due to non-Gaussian statistics [14]. This theory led to

$$\alpha = \frac{2}{3 - q}, \quad (4)$$

which we term the Tsallis relation. This quantifies a connection between anomalous diffusion and non-Gaussian statistics, predicting that a more highly non-Gaussian system (larger  $q$ ) will exhibit a greater degree of anomalous diffusion (larger  $\alpha$ ). In other words, particle random motion is predicted to be superdiffusive if the PDF is a non-Gaussian distribution with  $q > 1$ .

There are conflicting theoretical views on the validity of the generalized entropy that underlies the Tsallis relation, Eq. (4). On the one hand, there is an extensive theoretical literature based on the generalized entropy. These theories have been described as a successful new statistics that has the virtue of making a connection to the dynamics of a system [15]. On the other hand, in a critique it was argued that applying the generalized entropy leads to unphysical properties and that a temperature cannot be meaningfully measured if  $q \neq 1$  [16–18]. This conflict in the theoretical literature could be viewed either as a fundamental problem with the generalized entropy, or merely as a confusion arising from the use of the word “entropy” in the name of this quantity.

To help resolve a theoretical controversy like this, one useful approach of course would be to conduct experiments. We focus here on the Tsallis relation, Eq. (4), which can be tested experimentally in physical systems where random particle trajectories can be tracked. Equation (4) makes use of two measures,  $\alpha$  and  $q$ , which can both be determined from experimentally measured particle displacements. Any experimental system allowing these measurements will be of interest, especially when they yield measurements of particle motion that can be analyzed without relying on the same assumptions as the model. A definitive test of the Tsallis relation would require measurements of  $\alpha$  over a wide range of  $q$  as well as small random errors to provide a high significance level for the conclusion. We note that this test does not require measuring a temperature; it requires only measuring  $\alpha$  and  $q$ .

Two previous experimental comparisons to the Tsallis relation have been reported. One was the center-of-mass motion of hydra cells in cellular aggregates [19], where values  $\alpha = 1.24 \pm 0.1$  and  $q = 1.5$  were reported. Another was the motion of point defects in thermal convection patterns [20], where  $\alpha = 1.33$  was reported for observations over a narrow range of  $q \approx 1.5$ . Because these two experiments were performed for a narrow range of  $q$ , they do not permit a compelling test of Eq. (4). The authors are not aware of any other experimental comparison to the Tsallis relation.

A molecular dynamics simulation was performed to test a so-called  $\gamma$ - $q$  conjecture [21], which has the same form as Eq. (4). This system that was simulated consisted of particles at fixed positions with spins, lying in the  $x$ - $y$  plane, that interact. This simulation allowed varying  $q$  over a wide range. Different from our test here, the Tsallis  $q$  in [21] was estimated from velocity-autocorrelation function rather than the PDF as we used here.

### B. Approach for testing the connection

In this paper we will report experiments and simulations. These yield, as-fit parameters for the data, values for  $q$  and  $\alpha$ . These experiments and simulations do not rely on any of the assumptions underlying the Tsallis relation, for example, the assumptions that  $q$  is a measure of nonextensivity or that the generalized entropy is defined appropriately. By taking this approach, we intend to test the connection of anomalous diffusion and non-Gaussian statistics predicted by the Tsallis relation, without making use of the theory’s assumptions.

Ultimately, we will compare the observed deviations from normal diffusion and Gaussian statistics to determine whether they are correlated as predicted by the Tsallis relation.

We now introduce two quantities, representing deviations from normal diffusion and Gaussian statistics. First, we define a deviation from normal diffusion as

$$\delta_{\text{diff}} \equiv \alpha - 1. \quad (5)$$

Second, for a deviation from Gaussian statistics, instead of defining it as  $q-1$ , we are motivated by Eq. (4), to define it as

$$\delta_{\text{Gauss}} \equiv \frac{2}{3-q} - 1, \quad (6)$$

which is zero for Gaussian statistics,  $q=1$ , and increases with  $q$  over any reasonable range of  $q$ . Making use of these two definitions, the Tsallis relation, Eq. (4), can be rewritten as

$$\delta_{\text{diff}} = \delta_{\text{Gauss}}, \quad (7)$$

which is attractive for the purpose of testing using experimental and simulation results.

Our experiment makes use of a physical system that can be varied over a wide range of  $q$ . Random motion of particles can be tracked, and fitting the MSD and PDF yields experimental values for  $\alpha$  and  $q$ . Our physical system allows motion mainly in a two-dimensional (2D) plane without out-of-plane buckling. This allows direct imaging of all particles using a single camera, which simplifies the measurements. It also allows recording large data sets. Like many 2D systems, our experiment exhibits superdiffusion [5]. It also exhibits non-Gaussian statistics, with a fat-tail PDF that fits a Tsallis distribution, as we demonstrated previously [5]. In this paper, we will determine whether there is a correlation between the deviations from normal diffusion and Gaussian statistics,  $\delta_{\text{diff}}$  and  $\delta_{\text{Gauss}}$ , as an indication that non-Gaussian statistics and anomalous diffusion are connected.

Our experimental system is a single-layer dusty plasma. A dusty plasma is an ionized gas containing small particles of solid matter, which are negatively charged by collecting electrons and ions from a plasma [5,22–27]. The particles interact with a Yukawa repulsion [28], which is a soft potential allowing particles to interact most strongly with nearest neighbors but also with particles farther away. Particles are electrically confined into a single layer, forming a 2D suspension. As they move, particles experience a frictional drag in an ambient rarefied neutral gas. Direct imaging using video microscopy allows the tracking of particles [30] in the camera's field-of-view (FOV) so that random motion can be measured and characterized by using the MSD and PDF.

Unless we disturb the suspension, it almost never has an out-of-plane particle in the camera's FOV. The single-layer suspension is extremely soft, with a compressional sound speed of only 20 mm/s. Due to this extreme softness, if we disturb the suspension by laser heating (described below), a single out-of-plane particle can occasionally appear in an incomplete second layer and disturb the main layer by moving rapidly [29]. In preparing the experiment, we made efforts to

eliminate out-of-plane particles before applying laser heating. During laser heating, those out-of-plane particles appeared occasionally; when this resulted in a significant disturbance to the main layer we excluded those data, so that the conditions we analyze are more representative of steady-state conditions.

Some of the experimental results presented here are based on the same experiment as in Ref. [5]. There are four primary differences in the way we use the experimental data, as compared to [5]. First, we have analyzed data for many more conditions, yielding more data points for  $\alpha$  and  $q$ . We also performed a second experiment at a different gas pressure. Second, we use this larger data set to graph  $\delta_{\text{diff}}$  vs  $\delta_{\text{Gauss}}$  to test for a correlation in these measures, as predicted by the Tsallis relation, Eq. (7). Third, we exclude from our analysis any time series where random particle motion was significantly disturbed by an out-of-plane particle. Fourth, we compare this nonequilibrium experiment to new simulations we have performed to model equilibrium systems.

In the experiment, our dusty plasma is a driven-dissipative system. The particle kinetic temperature, in steady state, is set by a balance of driving forces and dissipation due to neutral gas friction.

In the absence of laser heating, the particles self-organize in a crystalline lattice structure due to the strong interparticle Coulomb interaction. Under these conditions, the only driving forces are believed to be a combination of Brownian kicks from neutral gas atoms and electrostatic fluctuations that arise from natural instabilities due to ion flow. When we apply laser heating, the particles experience strong kicks and the kinetic temperature rises sufficiently so that the crystalline lattice is disturbed. At modest laser powers this results in a liquid structure, which can be heated further by applying even higher laser powers. We will use data for the liquid structure to test for correlation of anomalous diffusion and non-Gaussian statistics.

We will find that in this 2D nonequilibrium experiment, as we vary the kinetic temperature, the measures of deviation  $\delta_{\text{diff}}$  from normal diffusion and  $\delta_{\text{Gauss}}$  from Gaussian statistics will vary. This allows us to compare these deviations and to test for a correlation indicating a connection between anomalous diffusion and non-Gaussian statistics.

We also report simulation results for a 2D equilibrium system that exhibits superdiffusion. As expected for the equilibrium system, it lacks non-Gaussian statistics. The simulations were performed with a kinetic temperature high enough to yield a liquid structure.

In addition to reporting values for  $q$  and  $\alpha$ , we also report a temperature for both experiment and simulation. Our approach here is to report a phenomenological value for the particle kinetic temperature, based on measurements of particle velocities as determined by particle displacements over a brief time  $\Delta t_f$ . Here, for two-dimensional motion, we will report

$$T = m \overline{(v_y - \bar{v}_y)^2}, \quad (8)$$

where  $m$  is particle mass,  $v_y = [y(\Delta t_f) - y(0)] / \Delta t_f$ , and the bar indicates an average over particles. We calculate this temperature separately for  $x$  and  $y$ , and for the experiment we

will report  $T$  calculated using only  $v_y$ . We note that for a nonequilibrium system, it has been argued that a kinetic temperature  $T$  measured in this way may not have the same physical meaning as a theoretical thermodynamic temperature [16,17]. In any case, our temperature measurements here are not central to this paper because they are not required for our test of the Tsallis relation. We use  $T$  for only one limited purpose: To characterize how far from equilibrium a system is, as indicated by fluctuations in  $T$ .

### III. EXPERIMENT METHOD

Here we review the experimental setup and procedures, which were presented in more detail in Ref. [5]. The apparatus, Fig. 1(a) of Ref. [5], centered on a vacuum chamber filled with a partially ionized argon gas. We introduced  $>6000$  polymer microspheres of  $4.83 \pm 0.08 \mu\text{m}$  in diameter. These microspheres experienced a frictional drag on the gas with a damping rate  $\nu_E$  [31]. The microspheres acquired a negative charge  $Q/e$ . Particles were electrically levitated in a single horizontal layer. The interparticle interaction in this type of single-layer dusty plasma has been found to obey a Yukawa potential [28], characterized by a screening length  $\lambda_D$ . The particle areal density was measured to determine the characteristic spacing  $a$ , termed the Wigner-Seitz radius [32]. Combining  $Q$  and  $a$ , we calculated a characteristic time scale for collective particle motion,  $\omega_{pd}^{-1}$ . We performed experiments under two conditions. For our main experiment, we used 8.6 mTorr argon gas pressure. Parameters for this main experiment were  $\nu_E = 2.5 \text{ s}^{-1}$ ,  $Q/e = -5700$ ,  $\lambda_D = 0.21 \text{ mm}$ ,  $a = 0.24 \text{ mm}$ , and  $\omega_{pd}^{-1} = 9.2 \text{ ms}$ . In this main experiment, we performed laser heating at 11 different laser powers in the range  $0.43 \leq P_L \leq 4.2 \text{ W}$ . Additionally, to check for consistency in our results, we performed a second experiment using 12 mTorr argon pressure. This was done for three different laser powers in the range  $2.6 \leq P_L \leq 4.2 \text{ W}$ , yielding less data, which we will use to check for consistency with the result of our main experiment. For the second experiment, parameters were  $\nu_E = 3.5 \text{ s}^{-1}$ ,  $Q/e = -6200$ ,  $\lambda_D = 0.20 \text{ mm}$ ,  $a = 0.24 \text{ mm}$ , and  $\omega_{pd}^{-1} = 8.2 \text{ ms}$ .

Particle trajectories were measured by tracking particles using video microscopy. We used a horizontally swept argon laser beam to illuminate particles, which we imaged from a top-view camera operated with an interval between frames  $\Delta t_f = 0.018 \text{ s}$ . To allow precise measurement of particle positions from the camera images using the moment method [30], we used a cooled camera, with a slightly defocused lens, and bright illumination. We verified in a test that the precision of our position measurements was so high that it had no detectable effect on the MSD. We tracked particles from frame to frame, yielding particle trajectories, i.e., threads, as shown in Fig. 1.

We used a large data set so that we can arrive at a significant conclusion, despite random scatter in our final graphs. We recorded movies of particle motion at 14 different heating laser powers. Each movie had either 2065 or 5500 frames. Altogether we made  $>2 \times 10^7$  measurements of particle positions.

Our experimental system is driven dissipative. Two laser beams move about on the suspension, kicking at any given

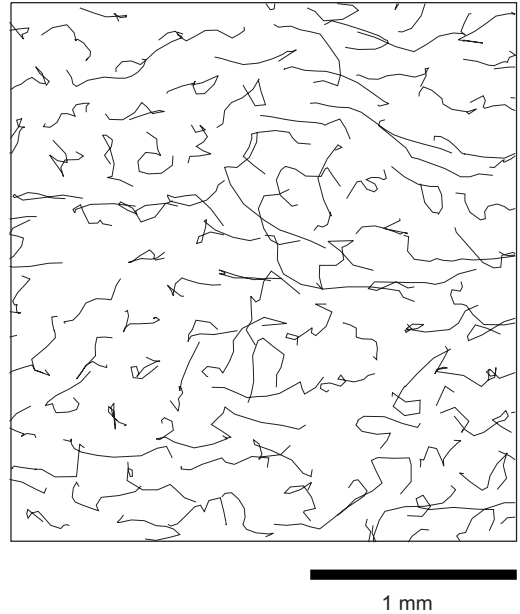


FIG. 1. Particle trajectories in our main experiment, for a suspension with liquid structure, at the heating laser power  $P_L = 4.2 \text{ W}$  and temperature  $T = 51\,000 \text{ K}$ . Trajectories shown here are for one cell, representing 1/6 of the camera's full field-of-view (FOV), for a time interval of 0.22 s. We use much longer trajectories to calculate the MSD (mean-square displacement) and PDF (probability distribution function).

time a few particles in the  $\pm x$  directions [33]. The kicked particles collide with other particles to thermalize their motion, increasing the kinetic temperature of the suspension. A steady state is achieved, as the energy dissipation to the neutral gas is balanced by the energy input from the heating laser as well as the Brownian kicks from neutral gas atoms and the natural instabilities in the dusty plasma. Particles are deflected more often by collisions with other particles than by the laser beams. As compared to the  $x$  direction, particle motion in the  $y$  direction is less affected by the strong kicks from the heating laser. Therefore, in using the experimental data we will analyze only the particle motion in the  $y$  direction in computing the PDF, MSD, and  $T$ .

Our experiment had some nonideal aspects arising from the laser heating, chiefly a nonuniformity in the kinetic temperature, and coherent modes in particle motion. We describe these next.

The temperature had both spatial and temporal fluctuations due to the rastered motion of our laser beams, which at any given time disturbed only small portions of the suspension. Averaged over the finite time of our movie, we find a spatial variation. The most extreme spatial variation was for our highest laser power, where the temperature in the hottest portion of the FOV was 35% higher than in the coldest. To reduce the effect of the spatial variation in our data analysis, we will partition our full FOV into six cells. Each cell corresponds to a smaller portion of the suspension, with a more uniform temperature than in the full FOV [5].

In addition to the desired random incoherent motion, particle motion also exhibited some intermittent mild oscillations at two frequencies, due to nonlinear combinations of

the laser-rastering frequencies [33]. We characterized the magnitude of this coherent motion by calculating the velocity power spectrum. We found that the power concentrated in the coherent modes was  $<10\%$  and  $<6\%$  of the total power for the  $x$  and  $y$  directions, respectively. In a test, we verified that these coherent modes had no significant effect on the conclusions of this paper. This test was done by numerically filtering the time series for particle positions to remove the two narrow frequency ranges containing most of the coherent motion. In this test we recomputed the MSD and PDF and there was no significant effect. We also recomputed  $q$  and  $\alpha$ , and we found that this changed their value only by a small amount, as compared to the scatter in the data.

## IV. DATA ANALYSIS METHOD

### A. Particle trajectories

We analyze the particle trajectories in the experiment to find the MSD and PDF, which we will use to quantify the deviations  $\delta_{\text{diff}}$  and  $\delta_{\text{Gauss}}$  from normal diffusion and Gaussian statistics, respectively. Here we provide greater detail for our analysis methods, which are the same as in Ref. [5], except that we now include far more data to allow a meaningful test of correlation of  $\delta_{\text{diff}}$  and  $\delta_{\text{Gauss}}$ .

#### 1. MSD

We calculated an MSD time series separately for each cell and laser power. An example of such a time series can be found in Fig. 2 of Ref. [5]. Each data point in this time series is for a given time  $\Delta t$ . Because measuring superdiffusion from MSD time series can be very sensitive to noise arising from limited numbers of threads, we used as much data and averaging as was practical. We computed each data point in the time series by averaging the square displacement not only over threads, but also over different overlapping time segments of the threads [34]. To further reduce noise, we averaged over all the available movies at a given laser power, which numbered from 18 to 30. The number of threads per movie was typically in the range 814 to 2000, corresponding to our lowest and highest laser powers, respectively. (While the number of particles in the FOV did not change, the number of threads identified by our software varied significantly for different laser power because the lifetime of a thread varied with laser power [5].) In the end, each data point in the MSD time series was the result of averaging a large number of values, for example, 1791 and 876 values for  $\Delta t = 1$  and 5 s, respectively, in our main experiment.

To quantify the deviation from normal diffusion, we fitted the averaged MSD time series in the range  $108 \leq \Delta t \omega_{pd} \leq 540$  to a power law, Eq. (3). This time interval was  $1 \leq \Delta t \leq 5$  s for our main experiment and  $0.88 \leq \Delta t \leq 4.4$  s for our second experiment. This fitting yielded a value for the exponent  $\alpha$ , which corresponds to one data point in Fig. 3(b). The scatter in the data in Fig. 3(b) is due to the finite numbers of movies and threads per movie.

#### 2. PDF

We calculated the PDF for various time intervals  $\tau$ , and we repeated this for each cell and laser power. We performed

these calculations for  $>200$  different time intervals  $\tau$ , in the range  $108 \leq \Delta t \omega_{pd} \leq 540$ . Because the non-Gaussian statistics that we hope to detect must be found in the large-displacement tail of a distribution, where the number of counts in a histogram are small, it is again necessary to use as much data and averaging as practical. As in the case of the MSD, we averaged over threads, then over overlapping time segments for each thread, and then over movies. Figure 2 shows three examples of the PDF chosen from the  $>200$  values of  $\tau$ , for  $P_L = 4.2$  W and  $T = 51\,000$  K.

To quantify the deviation from Gaussian statistics, we fitted PDF curves to the Tsallis distribution, Eq. (2), yielding a value for  $q$ . This value of  $q$  was for a specific  $\tau$ , and it was repeated for various beginning points in time series for a thread. It was also repeated for  $>200$  lengths for the time intervals, yielding  $>200$  values for  $q$ . Averaging these  $>200$  values yielded one measurement for  $q$  for each cell and laser power, which corresponds to one data point in Fig. 3(a).

The final step of our analysis is to prepare a graph comparing  $\alpha$  and  $q$ , Fig. 4. Recall that we varied  $\alpha$  and  $q$  by varying the laser power. We discuss Fig. 4 in detail, later.

### B. Temperature fluctuations

Because our experiment was done with a nonequilibrium system, and we will compare it to simulations intended to model equilibrium systems, it is useful to quantify how far from equilibrium a system was. We do this by recording a time series for the kinetic temperature  $T(t)$ , calculated from Eq. (8), and averaging the spatial-temporal variations over space to yield only the time variation. We then characterize the fluctuations of this spatially averaged kinetic temperature about its mean. For equilibrium systems, these temporal fluctuations arise from the finite number of particles,  $N$ . The fluctuations are expected in general to be larger for a nonequilibrium system, so that temperature fluctuation serves as a nonequilibrium indicator. For both the experiment and simulation, we began with a time series for the spatially averaged kinetic temperature,  $T(t)$ , calculated from the mean-square velocity fluctuation. We then calculated  $\delta T$  and  $\bar{T}$ , the rms fluctuation of  $T(t)$  and average over time. The observed fluctuation  $\delta T$  should be compared to a canonical fluctuation,  $\bar{T}(2/N)^{1/2}$ , which is the theoretical fluctuation for a finite-size 2D system in thermal equilibrium [35]. For the experiment, this was done separately for each cell, using the time series  $T(t)$  recorded for each frame in a movie. For the simulation, described in Sec. V, we used all the particles in the simulation box. The outcome of this test is a ratio  $\delta T / \bar{T}(2/N)^{1/2}$  of the observed fluctuation to the canonical fluctuation.

## V. SIMULATION METHOD

To demonstrate that, in contrast to the experiment, some systems have anomalous diffusion where  $\alpha$  is unrelated to  $q$ , we performed two kinds of numerical simulations. Both simulations represent equilibrium systems, in contrast to the experiment which is driven dissipative. The first kind of simulation is molecular dynamics (MD), and the second is

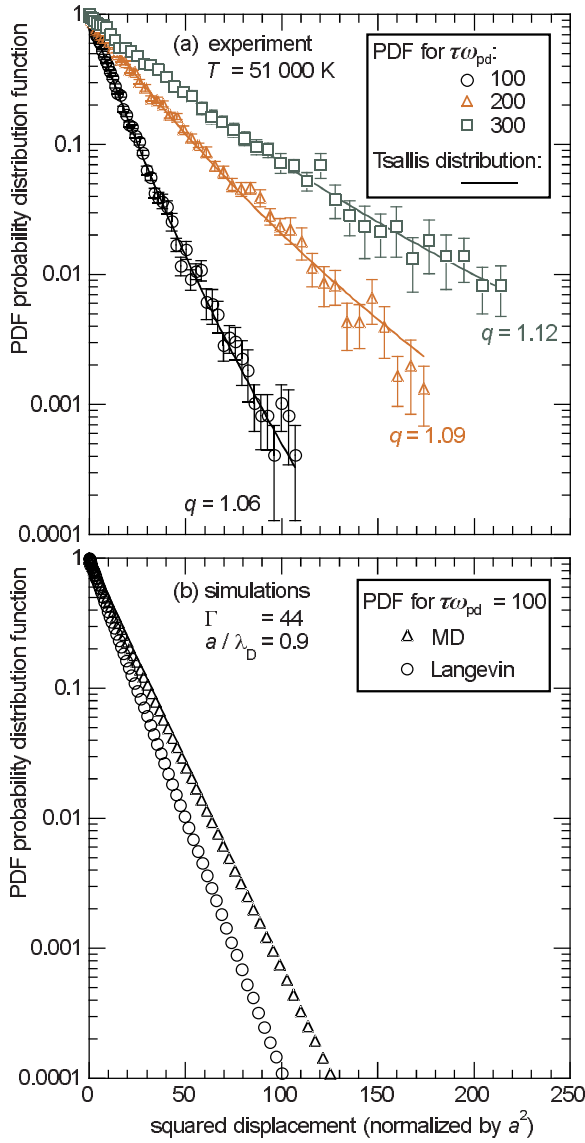


FIG. 2. (Color online) PDF for particle displacement. (a) Our main experiment, with nonequilibrium conditions. Data shown here are for three time intervals,  $\tau$ . Using a logarithmic scale for PDF plotted vs the squared displacement, a Gaussian function would be a straight line; here, the PDF is non-Gaussian with a fat tail. The smooth curves, from fitting to Eq. (2), yield values for  $q$ . Averaging all values of  $q$  for various time intervals, including the three shown here and 197 more in the range from 1 to 5 s, yields a measurement for  $q$  for one movie and one data point in Fig. 3(a). (b) Equilibrium simulations, for a  $\Gamma$  corresponding to the experimental temperature in (a), are nearly Gaussian. The experimental kinetic temperature  $T$  is computed using Eq. (8), and can be varied by adjusting the laser power. Data shown here are for a liquid structure.

Langevin dynamics (LD). These simulate frictionless and frictional systems, respectively.

In both kinds of simulation we used the same interparticle potential, boundary conditions, particle number and initial conditions, and diagnostics. The particle interaction was a binary repulsive Yukawa potential,  $\phi(r) = Q^2 \exp(-r/\lambda_D)/4\pi\epsilon_0 r$ . The boundary conditions were periodic, so that a particle exiting one side of the simulation box

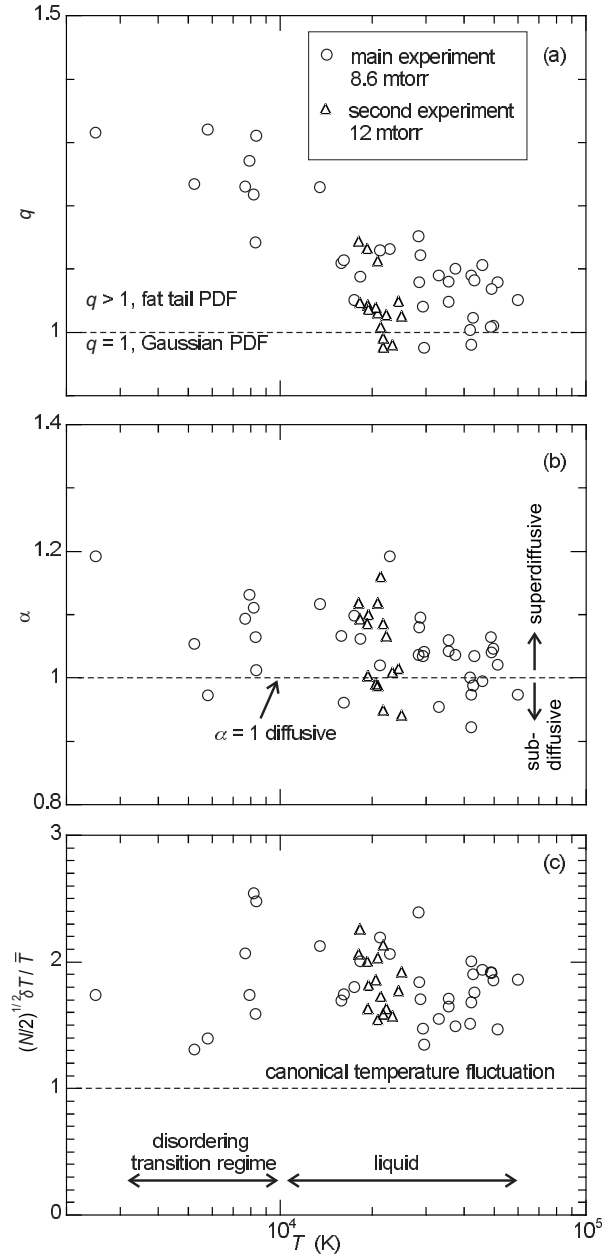


FIG. 3. Experimental results. Each data point corresponds to one cell in one movie, at one  $P_L$ . (a) The fit parameter  $q$  would be unity for Gaussian statistics, while our fat-tail PDF has  $q > 1$ ; i.e., this driven-dissipative system exhibits non-Gaussian statistics. (b) Diffusion exponent  $\alpha$ , as calculated by fitting the MSD to a power law. Normal diffusion has  $\alpha = 1$ , while anomalous diffusion has  $\alpha \neq 1$ . (c) Temperature fluctuations for the experiment. For an equilibrium system, the ratio would be unity. Temperature fluctuations can arise from finite-size effects [characterized by the “canonical fluctuation,”  $(2/N)^{1/2}\bar{T}$ ] and due to nonequilibrium effects. Here, the fluctuations exceed the “canonical fluctuation level,” which is an indicator of a nonequilibrium system.

reentered on the opposite side. We used  $N = 16\,384$  particles, which we started at random positions. We began recording time series data for particle positions and kinetic temperature after waiting  $3800 \omega_{pd}^{-1}$  to achieve equilibration. In a test, we repeated a simulation for two different initial configurations

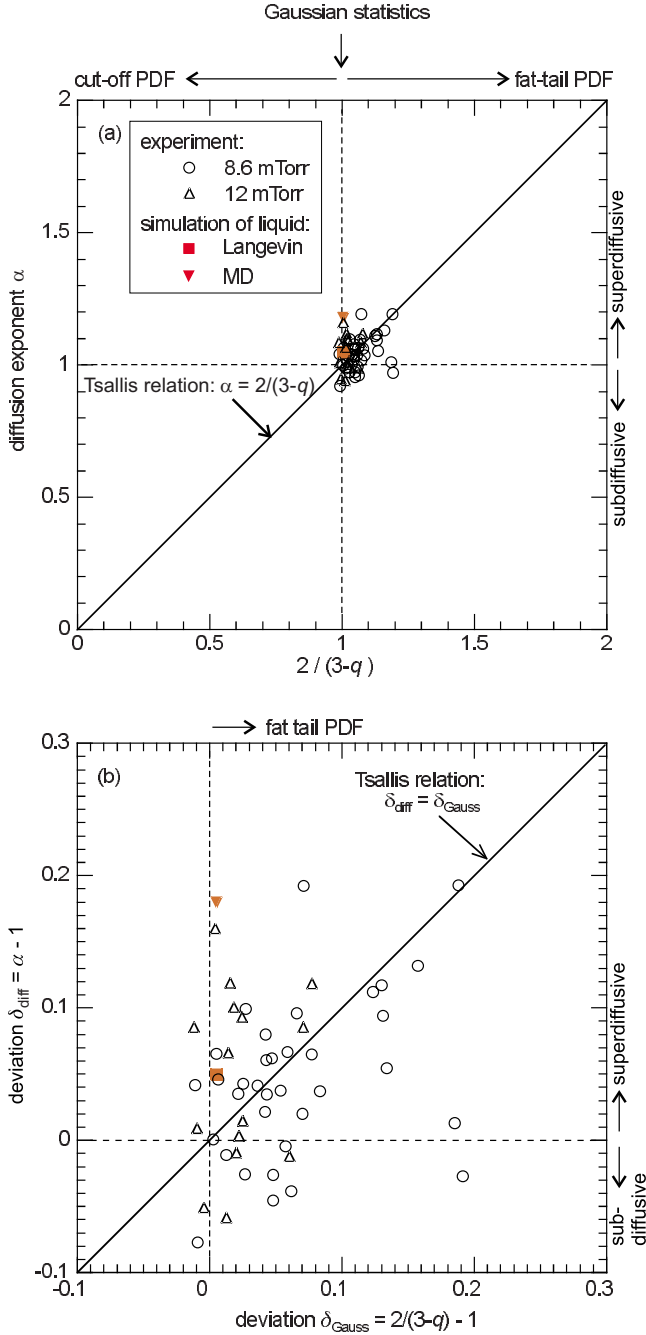


FIG. 4. (Color online) Correlation of superdiffusion with non-Gaussian statistics. (a) Variation of  $\alpha$  vs  $2/(3-q)$ . (b) For a more meaningful test of correlation, we plot the data with shifted origin so that the deviation from normal diffusion  $\delta_{\text{diff}} = \alpha - 1$  is plotted vs the deviation from Gaussian statistics  $\delta_{\text{Gauss}} = 2/(3-q) - 1$ . Note that for simulations, which modeled 2D thermal equilibrium systems, superdiffusion is not connected to non-Gaussian statistics, unlike the experiment, which was driven dissipative.

of the particle positions, and we found that the results were very close for both the MD and LD simulations. We used the same diagnostics as in the experiment, Sec. IV, except that we did not divide our simulation region into smaller cells. The following dimensionless parameters were chosen to mimic the run in our main experiment with  $T_y = 51\,000$  K:

The Coulomb coupling parameter was  $\Gamma = Q^2 / (4\pi\epsilon_0 a k_B T) = 44$ , and the screening parameter was  $a/\lambda_D = 0.9$ . These parameters correspond to a liquid structure.

In our MD simulation, we integrated the particle equation of motion,

$$m\ddot{\mathbf{r}}_i = -\nabla \sum \phi_{ij}. \quad (9)$$

A Nosé-Hoover thermostat was applied to control the temperature. Further details of our MD simulation method can be found in Ref. [13].

In our LD simulation, we integrated the Langevin equation of motion,

$$m\ddot{\mathbf{r}}_i = -\nabla \sum \phi_{ij} - \nu_E m \dot{\mathbf{r}}_i + \zeta_i(t). \quad (10)$$

Here,  $\nu_E m \dot{\mathbf{r}}_i$  is frictional drag, and  $\zeta_i(t)$  is a random force. At each time step a random force  $\zeta_i(t)$  computed from a Gaussian distribution with a zero mean and a magnitude chosen to satisfy the fluctuation-dissipation theorem,  $\zeta_i(0)\zeta_i(t) = 2m\nu_E k_B T_{\text{ref}} \delta(t)$ , according to a specified target temperature,  $T_{\text{ref}}$ . This random force models a stationary Markovian process. A random number was selected at each time step, for each particle, from the Gaussian distribution, without correlations with prior velocities or with the interparticle forces.

In a test of the simulations, we verified that the fluctuations of kinetic temperature were as expected for a system in equilibrium. We found that the ratio  $\delta T / \bar{T} (2/N)^{1/2}$  was 0.99 and 0.98 for our MD and Langevin simulations, respectively. While a ratio of unity would be ideal, a ratio within a few percent of unity as in our case is considered successful for molecular dynamic simulations of liquids using a thermostat [35]. This standard test gives us confidence that the simulations accurately mimic a system in thermal equilibrium.

## VI. RESULTS

### A. Experiment

#### 1. Temperature fluctuations

The fluctuations of kinetic temperature in the experiment confirm that the system is nonequilibrium. In Fig. 3(c), we see that the ratio  $\delta T / \bar{T} (2/N)^{1/2}$  exceeds unity. If our system were in thermal equilibrium and had a canonical ensemble fluctuation, the ratio  $\delta T / \bar{T} (2/N)^{1/2}$  would be unity; however,  $\delta T / \bar{T} (2/N)^{1/2}$  was typically larger by a factor of 2 or more in our experiment. This serves as a quantitative measure of how far from thermal equilibrium the experimental system was.

Examining the time series for temperature, we found that the instantaneous temperature fluctuated around a constant and did not have a universal upward or downward trend, for most of our data. This indicates that our experiment has reached a nearly steady state or dynamic equilibrium. The main exception to this was the occasional appearance of an out-of-plane particle that moved rapidly and disturbed the main layer; we excluded such data from analysis, so that the results we report are for two-dimensional motion under nearly steady-state conditions.

## 2. Non-Gaussian statistics

As reported in Ref. [5], particle random motion in our nonequilibrium experimental system exhibits non-Gaussian statistics. We found that the PDF fits the Tsallis distribution. In Fig. 2, we present the PDF graphed with the squared displacement as the horizontal axis so that the deviation from a Gaussian distribution can be more easily identified. By performing a least-squares fit to data as shown in Fig. 2, we found a value for  $q$  for each cell and each laser power; this was repeated for many different time intervals  $\tau$ , not just the three presented in Fig. 2(a), as explained in Sec. IV.

The deviation from a Gaussian distribution is characterized by  $q$ . We found that varying the laser power, and therefore the kinetic temperature, allowed us to vary  $q$ . In the absence of laser heating, the particles self-organized in a crystalline lattice, and we found  $q=1.5$ . Applying laser power to heat the suspension, we found that  $q$  trends downward at higher temperatures, approaching unity at the highest temperatures that we attained. This inverse trend of  $q$  with  $T$  is observed over a wide range of temperature, spanning the crystalline solid found at low temperature, the liquid at high temperature, and the disordering transition regime in between, as indicated in Fig. 3.

The inverse trend for our data in Fig. 3(a) is reminiscent of, but does not fit, a law  $q-1 \propto 1/(U_0/E_r)$  that was theoretically [37] predicted, and experimentally [38] observed in optical lattices, where  $U_0$  characterizes the strength of a confining potential and  $E_r$  is an atomic recoil energy. We do not have a detailed understanding of why  $q$  varies with laser power in the manner that is observed in this particular system, but it is useful that we are able to vary  $q$ , in order to enable a comparison to the Tsallis relation.

We note that the largest value of  $q$  is well below  $5/3$ , the largest value of  $q$  for which a PDF has a finite variance. Lévy flights, for example, are characterized by  $q > 5/3$  [39]. Our system has significant non-Gaussian statistics, but not to the extreme of, for example, Lévy flights. The results for our second experiment are consistent with our main experiment, in the range of  $q$  that was observed.

To verify that non-Gaussian statistics observed here is not transient, we have examined the time series for  $q$  at different intervals. For all the laser powers and cells where we report results, the time series showed no conspicuous universal upward or downward trend of  $q$  with time.

## 3. Diffusion exponent

As reported in Ref. [5], particle random motion in our system exhibits a low but statistically significant level of superdiffusion over a wide range of temperature. Making use of our new analysis, using more data, here we present details in Fig. 3(b) of the temperature variation of the diffusion exponent  $\alpha$ . The general downward trend of  $\alpha$  with  $T$  is seen in Fig. 3(b), for our main experiment, over a wide range of laser power. Our data points are mostly above  $\alpha=1$ , indicating superdiffusion, with some scatter arising from finite data time. Results from the second experiment are consistent with the range of  $\alpha$  observed in the main experiment.

## 4. Correlation of superdiffusion and non-Gaussian statistics

We now prepare two graphs to test the correlation between superdiffusion and non-Gaussian statistics, as pre-

dicted by the Tsallis relation, Eq. (4). In Fig. 4(a), we graph  $\alpha$  vs  $2/(3-q)$ . The data in Fig. 4 has some scatter, arising from the finite time of each movie. We will examine Fig. 4, attempting to identify correlations between  $\alpha$  and  $q$ , despite this scatter.

In examining Fig. 4(a), it is important to consider that the origin has no particular significance, and it is located far from the data points, so that it is not particularly significant that the data points appear to be clustered about the line of unity slope passing through the origin. We believe that it is more meaningful to graph the data with a shifted origin that is meaningful for indicating deviations from normal diffusion and Gaussian statistics. We do this in Fig. 4(b), making use of the deviations introduced in Eqs. (5) and (6), by graphing the same data with  $\delta_{\text{diff}} = \alpha - 1$  on the vertical axis and  $\delta_{\text{Gauss}} = 2/(3-q) - 1$  on the horizontal axis. Plotted this way, an equilibrium system with Gaussian statistics would appear at the shifted origin, as indicated by the intersection of two dashed lines corresponding to normal diffusion  $\alpha=1$  and Gaussian statistics  $q=1$ . The prediction of the Tsallis relation, Eq. (7), appears as a straight line passing through the shifted origin.

Our chief result is that we observe a correlation between superdiffusion and non-Gaussian statistics in our 2D liquid. This correlation is seen in Fig. 4(b) as an upward trend in the dependence of  $\delta_{\text{diff}}$  on  $\delta_{\text{Gauss}}$ .

To quantify this correlation, we used linear regression to fit the data to a line passing through the origin of Fig. 4(b). Analyzing the resulting slope and its standard error using a two-sided student's  $t$ -test, we find a  $p$  value less than  $10^{-4}$  for our main experiment. Thus, we can reject the null hypothesis that the slope is zero at  $>99.9\%$  significance level. In our second experiment, which has less data and correspondingly larger errors so that it is useful mainly for confirming results from the main experiment, we find a  $p$  value of 0.053, and we reject the null hypothesis with  $>90\%$  significance level. Thus, we conclude that there is a correlation between the superdiffusion and the non-Gaussian statistics in our experimental system.

Beyond verifying that there is a correlation, i.e., that the slope is nonzero, a more challenging experimental test would be to determine whether the slope is unity, as predicted by the Tsallis relation Eq. (7). One might suggest that the Tsallis relation appears confirmed in our experiment, as seen from the agreement of many data points with the prediction of Eq. (7). However, the scatter in our data in Fig. 4(b) prevents us from making such a definitive conclusion. Experiments averaged over more data, to provide better fits, would be required for a definitive test of the Tsallis relation.

## B. Simulation

The main results for our simulation of a 2D equilibrium liquid are an observation of Gaussian statistics together with anomalous diffusion. These are based on the PDF and MSD, respectively, in the same way as in the experiment. We present these results next.

As would be expected for a system in thermal equilibrium, the particle motion in our simulations exhibits Gauss-

ian statistics. We verified this by calculating the PDF for both simulations, presented in Fig. 2(b). Note that the PDF appears to be a straight line, as would be expected for a Gaussian distribution, when plotted with semilogarithmic axes and the square displacement as the horizontal axis. Our PDF is so close to a Gaussian that fitting it to the Tsallis distribution yields  $q=1.007 \pm 0.001$ , for both simulations. Such a negligibly small deviation from  $q=1$  Gaussian statistics is as expected, for a simulation that accurately mimics a system in thermal equilibrium.

Even though our 2D simulations are for thermal equilibrium, they both exhibit superdiffusion. For the parameters that were simulated here, we found that the diffusion exponent  $\alpha$  was 1.18 and 1.05, for our MD and LD simulations, respectively. In our earlier MD simulations (with a smaller  $N$ ) [36], we showed that  $\alpha$  is consistently  $>1$  for a wide range of temperature. In general, it is possible for 2D systems in thermal equilibrium to exhibit superdiffusion, and some authors have even predicted that superdiffusion will always occur in 2D liquids [10,11].

Combining these results for  $q$  and  $\alpha$  in Fig. 4, we include data points for our two simulations of a 2D equilibrium system. These simulation data differ conspicuously from the result of the experiment, which used a nonequilibrium system. This comparison leads us to one of our main conclusions: A 2D system in equilibrium can exhibit superdiffusion without any significant non-Gaussian statistics. In other words, superdiffusion can arise in 2D for reasons that are unrelated to non-Gaussian statistics. In such a case, the Tsallis relation cannot be expected to apply.

## VII. SUMMARY

We have conducted experiments with a 2D nonequilibrium driven-dissipative system and simulations of a 2D equilibrium system. In the experiment, the system consisted of a suspension of electrically charged microspheres in a plasma, which experienced both frictional drag on rarified gas and external energy input from rastered laser beams. We tracked random particle motion, and calculated the time series for mean-square displacement (MSD) and a histogram of particle displacements (PDF). Fitting the MSD time series to a power law yields the diffusion exponent  $\alpha$ , where  $\alpha=1$  would be expected for normal diffusion, and  $\alpha>1$  indicates superdiffusion. Fitting the PDF to a  $\kappa$  function or equivalently a Tsallis distribution yields a fit parameter  $q$ , where  $q=1$  would be expected for equilibrium systems, while  $q>1$  is interpreted as an indication of non-Gaussian statistics.

We found that the experiment exhibited both superdiffusion with  $\alpha>1$  and non-Gaussian statistics with  $q>1$ . By adjusting the laser power used to heat the suspension, we varied  $q$  over a wide range. Doing this, we found that a more highly non-Gaussian system exhibits a greater degree of anomalous diffusion.

To test for a correlation between anomalous diffusion and non-Gaussian statistics, we defined two parameters,  $\delta_{\text{diff}}$  and  $\delta_{\text{Gauss}}$ , to quantify the deviations from normal diffusion and Gaussian statistics, respectively. We plot our final data as  $\delta_{\text{diff}}$  vs  $\delta_{\text{Gauss}}$ . Large data sets were used to provide a significant number of data points over a wide range of  $q$ , to allow a meaningful test of correlation.

We found, with  $>99.9\%$  significance level, that anomalous diffusion and non-Gaussian statistics were correlated in our main experiment with a 2D liquid. In other words,  $\delta_{\text{diff}}$  increases with  $\delta_{\text{Gauss}}$ , and despite the scatter we can verify with  $>99.9\%$  significance level that the slope is nonzero. This result is qualitatively consistent with the Tsallis relation, Eq. (7). However, we are unable to make a definitive quantitative test of the Tsallis relation, that the slope is unity. Such a test would require reduced random errors, which in our experiment arose from finite data sets.

We note that our finding of a correlation between anomalous diffusion and non-Gaussian statistics does not prove a causal relationship. We have not demonstrated that anomalous diffusion is caused by non-Gaussian statistics, or *vice versa*. It is possible that some other phenomenon is responsible for both the non-Gaussian statistics and anomalous diffusion that were observed in our experiment.

Our simulation of 2D equilibrium liquids exhibited superdiffusion without a deviation from Gaussian statistics. This result, which is entirely different from the nonequilibrium experiment, demonstrates that not all systems with anomalous diffusion can be described by the Tsallis relation. We suggest that there is a need for clarification, in the theoretical literature, to define the regimes of applicability of the Tsallis relation.

Future experimental work would be required for an exact test of the Tsallis relation, Eq. (4). Reduced random errors would be required to perform this test with a sufficient significance level. It would also be attractive to carry out experiments with other experimental systems, where non-Gaussian statistics might arise from mechanisms different from those in our experiment.

## ACKNOWLEDGMENTS

We thank F. Skiff, Jack Scudder, and C. Tsallis for helpful discussions. This work was supported by NASA and DOE.

- 
- [1] A. Einstein, Ann. Phys. **17**, 549 (1905).
  - [2] V. Plerou, P. Gopikrishnan, L. A. Nunes Amaral, X. Gabaix, and H. E. Stanley, Phys. Rev. E **62**, R3023 (2000).
  - [3] C. K. Peng, J. Mietus, J. M. Hausdorff, S. Havlin, H. E. Stanley, and A. L. Goldberger, Phys. Rev. Lett. **70**, 1343 (1993).

- [4] P. Bak, C. Tang, and K. Wiesenfeld, Phys. Rev. Lett. **59**, 381 (1987).
- [5] B. Liu and J. Goree, Phys. Rev. Lett. **100**, 055003 (2008).
- [6] J. D. Scudder, Astrophys. J. **398**, 299 (1992).
- [7] L. F. Burlaga and A. F.-Viñas, Physica A **356**, 375 (2005).

- [8] C. Tsallis, *J. Stat. Phys.* **52**, 479 (1988).
- [9] L. Borland, *Phys. Lett. A* **245**, 67 (1998).
- [10] M. H. Ernst, E. H. Hauge, and J. M. J. Van Leeuwen, *Phys. Rev. Lett.* **25**, 1254 (1970).
- [11] J. R. Dorfman and E. G. D. Cohen, *Phys. Rev. Lett.* **25**, 1257 (1970).
- [12] B. J. Alder and T. E. Wainwright, *Phys. Rev. A* **1**, 18 (1970).
- [13] B. Liu, J. Goree, and O. S. Vaulina, *Phys. Rev. Lett.* **96**, 015005 (2006).
- [14] C. Tsallis and D. J. Bukman, *Phys. Rev. E* **54**, R2197 (1996).
- [15] E. G. D. Cohen, *Physica A* **305**, 19 (2002).
- [16] M. Nauenberg, *Phys. Rev. E* **67**, 036114 (2003).
- [17] M. Nauenberg, *Phys. Rev. E* **69**, 038102 (2004).
- [18] C. Tsallis, *Phys. Rev. E* **69**, 038101 (2004).
- [19] A. Upadhyaya *et al.*, *Physica A* **293**, 549 (2001).
- [20] K. E. Daniels, C. Beck, and E. Bodenschatz, *Physica D* **193**, 208 (2004).
- [21] A. Rapisarda and A. Pluchino, *Europhys. News* **36**, 202 (2005).
- [22] H. Thomas, G. E. Morfill, V. Demmel, J. Goree, B. Feuerbacher, and D. Mohlmann, *Phys. Rev. Lett.* **73**, 652 (1994).
- [23] J. H. Chu and Lin I, *Phys. Rev. Lett.* **72**, 4009 (1994).
- [24] B. Liu, K. Avinash, and J. Goree, *Phys. Rev. Lett.* **91**, 255003 (2003).
- [25] V. Nosenko and J. Goree, *Phys. Rev. Lett.* **93**, 155004 (2004).
- [26] S. Ratynskaia, K. Rypdal, C. Knapik, S. Khrapak, A. V. Milovanov, A. Ivlev, J. J. Rasmussen, and G. E. Morfill, *Phys. Rev. Lett.* **96**, 105010 (2006).
- [27] S. Nunomura, D. Samsonov, S. Zhdanov, and G. Morfill, *Phys. Rev. Lett.* **96**, 015003 (2006).
- [28] U. Konopka, G. E. Morfill, and L. Ratke, *Phys. Rev. Lett.* **84**, 891 (2000).
- [29] D. Samsonov, J. Goree, Z. W. Ma, A. Bhattacharjee, H. M. Thomas, and G. E. Morfill, *Phys. Rev. Lett.* **83**, 3649 (1999).
- [30] Y. Feng, J. Goree, and B. Liu, *Rev. Sci. Instrum.* **78**, 053704 (2007).
- [31] B. Liu, J. Goree, V. Nosenko, and L. Boufendi, *Phys. Plasmas* **10**, 9 (2003).
- [32] G. J. Kalman, P. Hartmann, Z. Donkó, and M. Rosenberg, *Phys. Rev. Lett.* **92**, 065001 (2004).
- [33] V. Nosenko, J. Goree, and A. Piel, *Phys. Plasmas* **13**, 032106 (2006).
- [34] M. J. Saxton, *Biophys. J.* **72**, 1744 (1997).
- [35] B. L. Holian, A. F. Voter, and R. Ravelo, *Phys. Rev. E* **52**, 2338 (1995).
- [36] B. Liu and J. Goree, *Phys. Rev. E* **75**, 016405 (2007).
- [37] E. Lutz, *Phys. Rev. A* **67**, 051402(R) (2003).
- [38] P. Douglas, S. Bergamini, and F. Renzoni, *Phys. Rev. Lett.* **96**, 110601 (2006).
- [39] C. Tsallis, S. V. F. Levy, A. M. C. Souza, and R. Maynard, *Phys. Rev. Lett.* **75**, 3589 (1995).